Regular Article

ORGANIC CHEMISTRY RESEARCH
Published by the
Iranian Chemical Society
www.orgchemres.org

Org. Chem. Res., Vol. 6, No. 2, 242-256, September 2020.
DOI: 10.22036/org.chem.2020.228472.1242

Theoretical Study on the Interaction between 5-Fluorouracil Anticancer Drug and Nitrosamine as a Family of Potent Carcinogenic Compounds in Different Solvents: A Quantum Chemical Study

L. Hokmabadi[a,*] and A. Khanmohammadi[b]

[a]*Department of Chemistry, Payame Noor University, Tehran 19395-4697, Iran*
[b]*Young Researchers and Elite Club, Quchan Branch, Islamic Azad University, Quchan, Iran*
(Received 25 April 2020, Accepted 17 August 2020)

In this research, the effect of different solvents on the stability order, binding energy and hydrogen bond (H-bond) strength of Fluorouracil-Nitrosamine (FU-NA) complex is investigated by using the density functional theory. The calculations are conducted at the M06-2X/6-311++G(d,p) level of theory for geometry optimization of the complex and its monomers. Based on the average energies of the H-bonds calculated, the H-bond strength in the gas phase is higher than that in the solution phase. The H-bond average energies in polar solvents are close to each other and lower than those in the non-polar solvents. Our findings also show that when the solvent effect is applied the binding energy of complex is significantly changed. The binding energy in the solution phase is also lower than that in the gas phase. Therefore, the stability in the polar solvents with respect to the water as natural solvent is higher than that in the non-polar ones. The natural bond orbital analysis and the Bader's quantum theory of "Atoms in Molecules" are also applied to evaluate the H-bond interactions in the selected solvents.

Keywords: 5-Fluorouracil, Nitrosamine, Solvent effect, NBO, QTAIM

INTRODUCTION

Intermolecular forces play an essential role for explaining many phenomena in numerous areas of modern chemistry, from molecular biology to supramolecular chemistry [1-3]. The H-bond, in particular, is one of the most important intermolecular interactions present in different biological activities [4-8]. The study of H-bond systems is a subject of great interest since they have significant effect on the structure of compounds in the solid, liquid and gas phases [9,10]. The H-bonds are really a special case of dipole forces; however, they are usually stronger than normal dipole forces between molecules [11]. For H-bonded systems, the influence of the different solvents on the geometrical and topological parameters has been considered in many studies. For example, Roohi *et al.* [12] investigated the structure, stability and proton transfer in H-bonded complexes formed from interaction between uracil and parent nitrosamine using B3LYP, B3PW91 and MP2 methods with a wide range of basis sets. Yoosefian and co-workers [13] showed the effect of various solvents on the stability order, binding energy and H-bond strength of cytosine-guanine complex by using the density functional theory. In 2017, the nature and properties of H-bond interactions in adenine-thymine complex analyzed with quantum chemical calculations by Souri *et al.* [14]. A theoretical study of the interaction between the 5-fluorouracil anticancer drug with various nitrosamine compounds was also conducted in 2015 [15].

The Bader's quantum theory of "Atoms in Molecules" (QTAIM) offers a convenient means of looking at H-bonding interaction in various intermolecular systems [16]. One of the advantages of the AIM theory is that one can obtain information on the concept of chemical bond and the bond strength in terms of electron density distribution

*Corresponding author. E-mail: lhokmabady8223@gmail.com

function [16,17]. It exploits the topological features of electron density, and thereby, a definition of chemical bonding through bond path and bond critical point (BCP). A BCP (a point at which gradient vector vanishes, $\nabla\rho(r) = 0$) is found between the two nuclei of the molecule in equilibrium geometry, which is considered to be connected by a chemical bond. The topological descriptors obtained from the AIM theory and electron localization function can be successfully employed to distinguish weak, medium, and strong H-bonds in various molecular systems.

Organic solvents are often used as a vehicle to dissolve hydrophobic compounds in cell biology experiments [18-22]. They should be highly soluble and not have a toxic effect on the cells. For cell fixation, methanol and acetone solvents are applied [23]. Methanol is also most commonly used to fix frozen sections, cell culture cells or smears. This leads to preserve the cellular architecture and frozen tissue sections and cells. Alcohols can affect several neurotransmitter systems and cause significant changes in the brain. For instance, ethanol depresses the brain function, very much in the style of an anesthetic. At low blood concentrations, ethanol releases behaviors that are otherwise inhibited and usually causes feelings of relaxation and good mood which may facilitate socializing. The use of DMSO (dimethyl sulfoxide) is in the cell's freezing as well as cryopreservation [24], so it is essential to know that whether it can be effective on bonds and the structure of compounds or not. DMSO can be also applied as a solvent for chemopreventive agents [25]. For permeabilizing of cells before some tests, the ether is used. It is also applied as a constructor material in some synthetic medicinal compounds. The chloroform can reveal the most anticancer ability. Its extract from HDW (Hedyotis diffusa Willd) prevents the survival of cancer cells [26]. In addition, 70% of the cell volume is water, so it plays a vital role for all living things.

5-Fluorouracil (5FU) is the simplest chemotherapeutic drug which shows radio sensitizing activity [27]. This compound belongs to the class of organic compounds known as halopyrimidines. In other words, it is an aromatic compound containing a halogen atom linked to a pyrimidine ring. The 5FU is utilized for the treatment of the cancers such as the breast, rectum, colon, stomach, or the pancreas [28,29]. In addition to cancer, it is also used for a variety of other pharmaceutical purposes including porokeratosis and psoriasis, sun damaged skin and genital warts [30-32]. The complexity of its action mechanism, which is dependent on whether the tissue is tumor or normal, makes the drug very attractive for biochemical modulation regimens [33]. The ^{19}F NMR technique is widely used for in vitro detection of this drug. In ^{19}F NMR studies of 5FU chemotherapy [34,35], its signal often serves as an internal chemical shift standard. Furthermore, ^{19}F magnetic resonance spectroscopy (^{19}F MRS) is selected as the main tool to check 5FU and its conversions in tumor tissue. This method is used to study the 5FU retention and its metabolism both *in vitro* and *in vivo* [36].

Nitrosamine (NA) compounds are potent carcinogens reported by the International Agency for Research on Cancer [37]. They are chemical compounds with the functional group -N-N=O, a nitroso group bonded to an amine. The NAs are widespread in environment such as cigarette smoke, beer, bacon and diet. Furthermore, they can be produced in the stomach by reaction of secondary amines and nitrite (NO_2^-) both taken from foods, causing serious health hazards even in trace amounts [38-41]. Most NAs are carcinogenic. They can form DNA adduct to cause cancer in the human body [42]. While NAs can cause cancer, 5FU is a chemotherapy drug used to various cancers, including those linked to NAs like gastric cancer. The antitumor activity of a drug is related to its molecular properties as well as its interactions with different targets in cells. Because of the importance of 5FU in treating various types of cancers, the interaction between this drug with NA compounds and the effects of these interactions on their properties are very important. Furthermore, these complexes can be considered as model systems for understanding the H-bonding interactions in biomolecules.

The main goal of this study is to investigate the effect of different solvents on the stability order, binding energy and H-bond strength of the FU-NA complex and their results are compared with each other and also with the gas phase. The geometrical parameters, topological properties and natural bond orbital (NBO) analysis are also performed to gain further insight into the effect of intermolecular interactions on the H-bond strength.

COMPUTATIONAL DETAILS

In this study, all calculations are carried out using the Gaussian 03 program [43]. The obtained complex and their monomers are optimized using the M06-2X [44] method and the 6-311++G(d,p) (437 basis functions, 693 primitive Gaussians) basis set. The vibrational frequencies are calculated at the same level of theory on the optimized geometries. Frequency calculations indicate that the studied complex is in true minima (no imaginary frequency mode). The complex formation is investigated in the presence of various solvents with a wide range of dielectric constants (including water, methanol, ethanol, ether, chloroform, acetone and DMSO). The Tomasi's polarized continuum model (PCM) using the integral equation formalism variant (IEFPCM) is applied to follow the effect of different solvents [45-47]. Furthermore, the solvent effect on the complex stability order and the H-bonds are analyzed and their results are compared with each other and also with the gas phase. In this study, the approximate values of the intermolecular H-bond energies are estimated by the Espinosa-Molins method [48]. For the FU-NA complex, the binding energy (ΔE) is also calculated by evaluating the difference between the total energies of complex and the individual monomers, as given in Equation (1):

$$\Delta E = E_{FU\text{-}NA} - (E_{FU} + E_{NA}) \quad (1)$$

where $E_{FU\text{-}NA}$ is the total energy of complex, and E_{FU} and E_{NA} are the total energies of 5-fluorouracil and nitrosamine monomers, respectively. The binding energies are computed with correction for the basis set superposition error (BSSE) using the Boys-Bernardi counterpoise technique [49]. To get more information about the nature of the investigated interactions, a topological analysis is achieved to calculate the electron density (ρ) and its second derivative ($\nabla^2\rho$) at the bond critical point (BCP) by the AIM method [16,50,51]. The AIM analysis is performed using the AIM2000 program [52] on the optimized wave functions. Additionally, the natural bond orbital (NBO) [53] analysis, using the Gaussian 03 program, is done to better understand the intermolecular interactions. Both the AIM and NBO analyses are performed at the M06-2X/6-311++G(d,p) level of theory.

RESULTS AND DISCUSSION

Molecular Geometry and Energies

The obtained structures from the interaction between 5FU and NA are depicted in Fig. 1. For H-bond formation in the FU-NA complex, the NA can be placed in three regions in vicinity of the FU. According to our previous studies [54,55], among the various H-bonding sites, the A1 site of complex has the strongest interaction (see Fig. 1). Our findings show that the binding energies obtained for A1, A2 and A3 sites of complexes are -36.60, -24.49 and -25.50 kJ mol^{-1}, respectively. This means that the A1 site of complex is more stable than the A2 and A3 sites. Therefore, we used the most stable complex to examine the effect of different solvents on it. As it can be seen in Fig. 1, two kinds of H-bonding exist via the FU-NA interaction: N-H···O and C-H···O. It is obvious that both the FU and NA monomers can act simultaneously as proton donors and proton acceptors. Hence, the FU is expected to form a binary H-bonded complex with the NA. In this study, several different solvents representing environments of diverse polarity are chosen. In order to investigate the geometry and the intermolecular H-bond energy changes in the FU-NA complex, optimization in water, methanol, ethanol, ether, chloroform, acetone and DMSO solvents is carried out using M06-2X method and the 6-311++G(d,p) basis set. Furthermore, the influence of the solvent on the stability order of the FU-NA complex and the strength of intermolecular H-bonding is considered using the IEFPCM method.

The most important geometrical parameters and H-bond energies of the FU-NA complex calculated at the M06-2X/6-311++G(d,p) level of theory are given in Table 1. It is well known that the H-bond distances can be considered as a criterion of H-bonding strength. In other words, the shorter the length of the generated bridges between monomers (H-bond distances) can be attributed to the stronger the H-bond energies (E_{HB}). From Table 1, it is apparent that the estimated $O_{NA}\cdots H_{FU}$ and $O_{FU}\cdots H_{NA}$ distances are in the ranges 1.864-1.875 Å and 2.237-2.292 Å, respectively. Thus, the strongest bond is formed between O_{NA} and H_{FU} and the weakest bond is belonged to $O_{FU}\cdots H_{NA}$. This result clearly shows that the H-bond for the $O_{NA}\cdots H\text{-}N_{FU}$ interaction is stronger than that for the

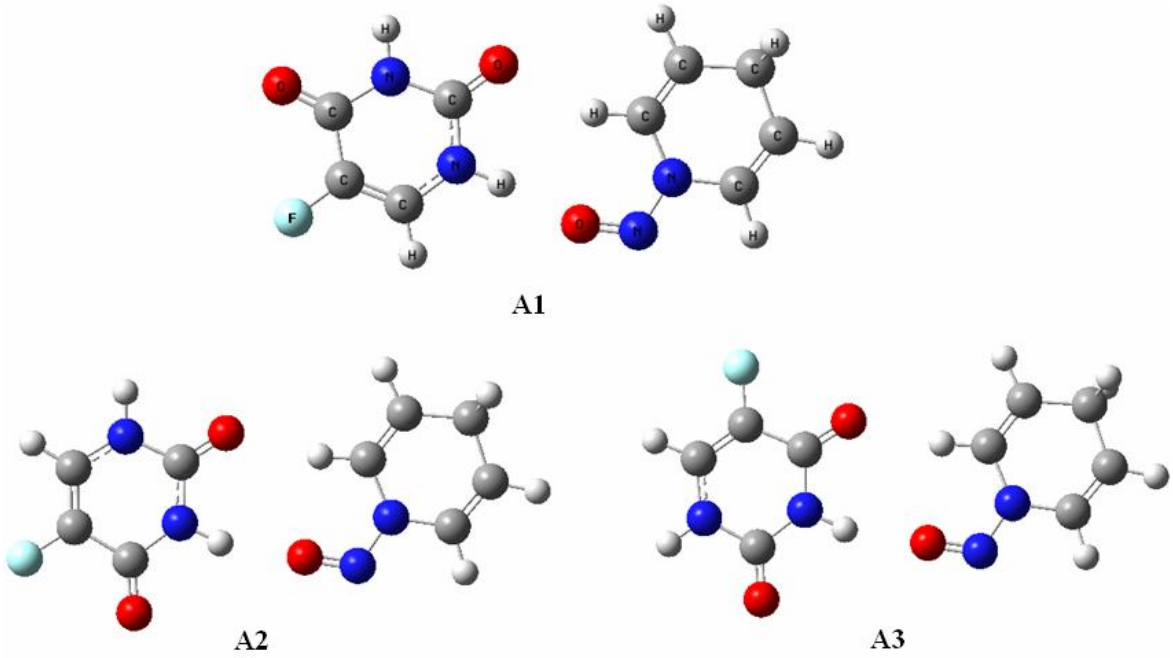

Fig. 1. The optimized structure of FU-NA complex in various sites of A1, A2 and A3.

Table 1. Geometrical Parameters of H-bonds (Bond Length in Å) and H-bond Energies (E_{HB} in kJ mol^{-1}) of FU-NA Complex in Different Solvents

Media	$N\text{-}H_{(FU)}$	$C\text{-}H_{(NA)}$	$O_{NA}\cdots H_{FU}$	$O_{FU}\cdots H_{NA}$	E_{HB} ($O_{FU}\cdots H\text{-}C_{NA}$)	E_{HB} ($O_{NA}\cdots H\text{-}N_{FU}$)
Water	1.019	1.079	1.875	2.292	-9.89	-27.58
DMSO	1.019	1.079	1.874	2.292	-9.90	-27.64
Methanol	1.019	1.079	1.873	2.292	-9.89	-27.69
Ethanol	1.019	1.079	1.873	2.292	-9.90	-27.72
Acetone	1.019	1.079	1.873	2.292	-9.90	-27.77
Chloroform	1.019	1.079	1.868	2.288	-10.04	-28.32
Ether	1.019	1.079	1.867	2.287	-10.05	-28.41
Gas phase	1.018	1.080	1.864	2.237	-11.65	-28.60

$O_{FU}\cdots H\text{-}C_{NA}$ one (see Table 1). In recent years, the powerful method of Espinosa [48] is often applied for the estimation of H-bond energy. In this method, the H-bond energies may be calculated approximately from the properties of bond critical points. First, the estimation of G(r) in terms of electron density ρ(r), its gradient $\nabla\rho(r)$ and its Laplacian

$\nabla^2\rho(r)$ functions is suggested by Abramov [56]. The procedure for obtaining G(r) at the critical point, where $\nabla\rho(r) = 0$, is as follows:

$$G(r_{CP)} = (\frac{3}{10})(3\pi^2)^{\frac{2}{3}}\rho^{\frac{5}{3}}(r_{CP}) + (\frac{1}{6})\nabla^2\rho(r_{CP}) \quad (2)$$

By using the virial equation, the local potential energy density $V(r_{CP})$ can be estimated [56], as given below:

$$2G(r_{CP}) + V(r_{CP}) = (\frac{1}{4})\nabla^2\rho(r_{CP}) \quad (3)$$

And finally, the relationship between H-bond energy (E_{HB}) and the potential energy density at O···H bond critical points $V(r_{CP})$ is presented as: $E_{HB} \approx \frac{1}{2}V(r_{CP})$

As shown in Table 1, the H-bond energies of the studied complex change when solvent effect is taken into account. Based on the average energies of the H-bonds calculated, the H-bond strength in the gas phase is more than that in the solution phase. The H-bond average energies in polar solvents are close to each other and lower than those in the non-polar solvents. The trend in the calculated H-bond energies in the different solvents is as follows:

Water ≈ DMSO ≈ methanol ≈ ethanol ≈ acetone < chloroform ≈ ether

As seen, the maximum and minimum values of the H-bond energy correspond to the non-polar and polar solvents, respectively. However, the highest value of the H-bond energy is observed in the ether solvent with respect to the other cases.

Our findings also show that when the solvent effect is applied the binding energies of complex are significantly changed. Table 2 summarizes the calculated binding energies in the H-bond formation process, where the binding energies are defined as the energy difference between the optimized complex and the sum of the individual monomers. Comparing the obtained binding energies with the H-bond energies of the FU-NA complex in the various solvents shows a direct relationship between them. In other words, the results show that the binding energy of FU-NA complex in the polar solvents is lower than that in the non-polar ones while it is higher than the solution in the gas phase.

Vibrational Frequencies

In continuation of our studies for a better elucidation of the H-bond strength, the vibrational frequencies are calculated for the FU-NA complex in the presence of different solvents. Table 2 shows the N-H and C-H bonds vibrational frequencies of the FU-NA complex relative to those of their monomers. The frequency shifts ($\Delta\upsilon$) are defined as the difference between the frequency of the certain vibrational mode in the complex and that in the isolated monomer and can be expressed as: $\Delta\upsilon = \upsilon_{complex} - \upsilon_{monomer}$. The obtained computations reveal that the vibrational frequencies of the N-H bonds involved in H-bonding are red-shifted, whereas those of the C-H bonds are blue-shifted. Result of calculations also shows that the N-H vibrational frequencies suffer the larger changes in the O_{NA}···H-N_{FU} H-bonds in comparison to the C-H vibrational frequencies in the O_{FU}···H-C_{NA} ones.

Our theoretical outcomes based on the N-H vibrational frequencies values ($\Delta\upsilon_{N-H}$) show that the studied complex in the polar solvents has the greatest red shift, whereas the least red shift belongs to the non-polar solvents. These results are reversed for vibrational parameters of C-H (υ_{C-H}). There is relatively good linear relationship between the C-H stretching frequencies ($\Delta\upsilon_{C-H}$) involved in the O_{FU}···H-C_{NA} H-bond with the binding energies. The correlation coefficient (R) for the dependency of ΔE *vs.* $\Delta\upsilon_{(C-H)}$ is equal to 0.872 with an equation as: $\Delta E = -4.7303\ (\Delta\upsilon_{C-H}) + 122.44$. This means that the stretching frequency values may be a useful parameter for describing the strength of the H-bond interactions in the studied complex. The infrared spectra of the FU-NA complex are also predicted theoretically from the calculated intensities (see Table 2). The infrared spectrum of FU-NA complex (related to C-H bond) in the non-polar solvents shows a weaker band compared to the polar ones. On the other hand, the strong infrared bands at about (1414-1461 cm^{-1}) is assigned to N-H stretching modes. As shown in Table 2, the highest IR values belong to the polar solvents, while the lowest values correspond to the non-

Table 2. Calculated Binding Energies (ΔE) in Terms of kJ mol^{-1}, Stability Order (S.O.), Dielectric Constant (ϵ) of the Solvents, Stretching Frequencies Information (Δυ, IR, Infrared, in cm^{-1}) of N-H and C-H Groups and Dipole Moment (μ, in Deby)

Media	ΔE	S.O.	ϵ	$\Delta\upsilon_{(N-H)}$	$\Delta\upsilon_{(C-H)}$	$IR_{(N-H)}$	$IR_{(C-H)}$	μ
Water	-15.51	0.00	80.0	-131.78	28.87	1460.76	103.38	9.48
DMSO	-15.79	0.31	46.8	-132.33	29.13	1460.10	103.41	9.46
Methanol	-16.09	0.64	32.7	-132.30	29.19	1459.36	103.21	9.43
Ethanol	-16.41	0.97	24.5	-131.09	29.36	1456.64	103.01	9.40
Acetone	-16.68	1.26	20.7	-131.34	29.48	1455.79	102.88	9.37
Chloroform	-21.69	6.62	4.81	-130.77	31.40	1419.19	101.84	8.89
Ether	-22.35	7.33	4.33	-130.88	31.52	1413.90	101.65	8.83
Gas phase	-36.60	22.47	-	-136.06	32.19	1178.42	106.22	7.25

polar ones. In fact, the strong infrared band of 1461 cm^{-1} in the water (as a polar solvent) moves to 1414 cm^{-1} in the ether (as a non-polar solvent). The upper frequency shift of this band in water (47 cm^{-1}) suggests more stretching character for N-H bond in the studied complex.

Stability Order and Dielectric Constant

In order to investigate the influence of solvent on the stability order of FU-NA complex, we have chosen water as a natural compound of the cells to compare its effect with the other solvents and also with the gas phase [13]. It is worth mentioning that 70% of cell volume is occupied with the water and it can change the H-bond characters such as energy, structure and electron density [13,57-61]. The stability order (S.O.) values of FU-NA complex obtained in the different solvents are collected in Table 2. According to the binding energies, the stability in the polar solvents is higher than the non-polar ones. Theoretical results reveal that the increment of stability of 5FU, NA and FU-NA complex in the polar solvents is accompanied with the decrease of formation energy of the FU-NA complex in these solvents (see Fig. 2). There is an excellent linear relationship between the calculated binding energies and the stability order. In other words, as the absolute binding energies increase, the stability order is found to decrease. The corresponding correlation coefficient (R) is equal to 1 and the equation of regression line is as follows:

$$\Delta E = -0.9388\ S.O. - 15.493$$

From the obtained data, it can be concluded that although the studied complex has the most binding energies in non-polar solvents, its stability in these solvents is lower than that in the others. As shown in Table 2, the FU-NA complex has the highest binding energy value and the lowest stability value in ether (as non-polar solvent).

The influence of solvents dielectric constant (ϵ) on the binding energy values is also analyzed. As it is obvious from Table 2, the increment of dielectric constant of the solvent is accompanied by decreasing the binding energy. Correlation between values of the binding energy versus the dielectric constant is shown in Fig. 3. The result of calculations indicates that the increase of solvent polarity causes to shift the binding energies toward less value. Therefore, the formation of FU-NA complex in the ether (as non-polar solvent), is more favorable with respect to the other solvents, energetically. The effect of solvent dielectric constant on the stability order is also investigated. Figure 3 reveals the correlation between the dielectric constant and the stability order. As shown in Table 2, by increasing the

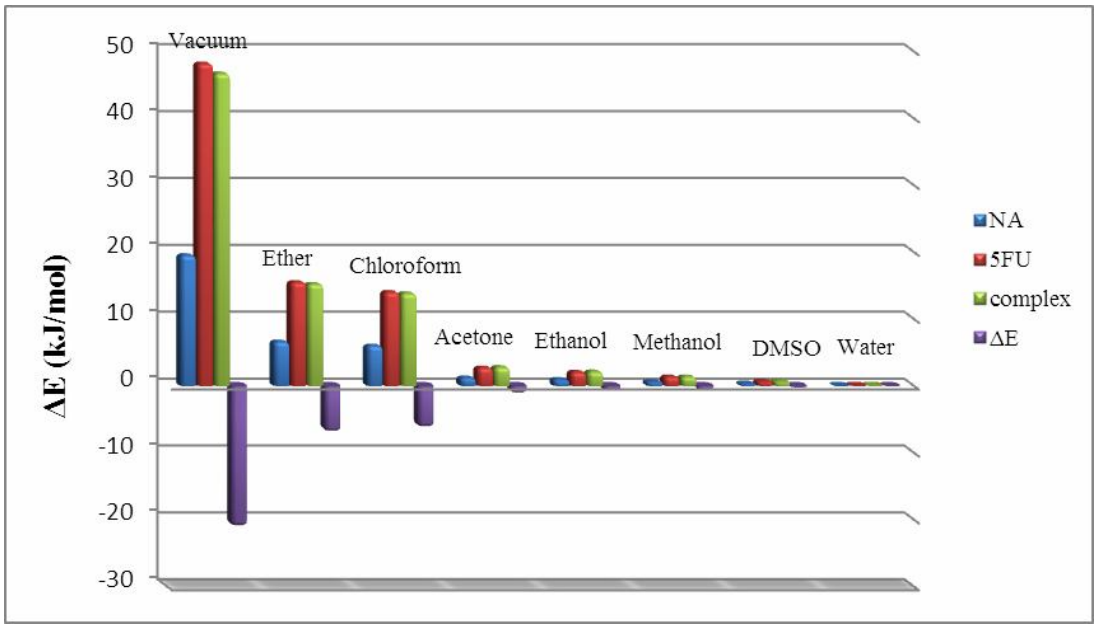

Fig. 2. The correlation between the stability order and the binding energy of 5-fluorouracil, nitrosamine and FU-NA complex.

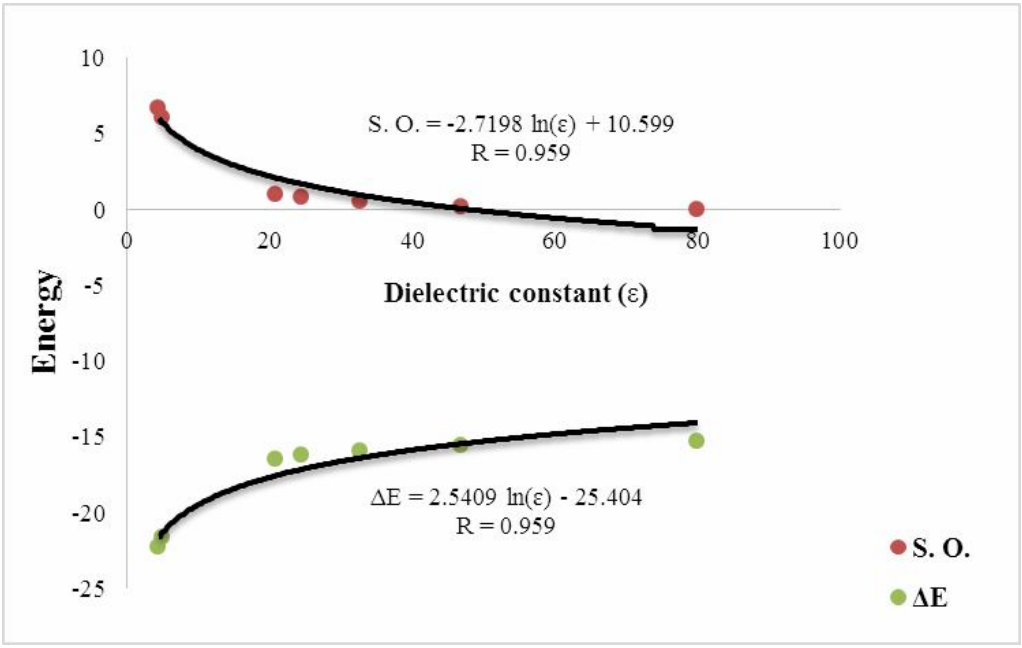

Fig. 3. The relationship between stability order (S. O.) and binding energy (ΔE) *versus* the solvents dielectric constant (ϵ).

solvent dielectric constant, the stability of the FU-NA complex increases. Hence, the most stable structure is perceived in the water solution; as a result, the stability order in the studied system depends on the solvent type.

The dielectric constant values can also affect on the dipole moment of FU-NA complex. The obtained results show that the calculated dipole moments (μ) in the various solvents are quite large (see Table 2). It is worth mentioning that a major factor in the energetic and dipole moment of a wide variety of compounds is solvation. The field generated by the surrounding solvent perturbs the structures and induces a dipole moment in the molecule. Since, the dipole moment (μ) is achieved from the sum of the permanent (μ_o) and induced parts, so, it is predicted that molecular dipole moment increases in solution [62,63]. Furthermore, the large dipole moments demonstrate the high reactivity of molecules. This enhancement is due to the charge distribution and migration from one region of molecule to the other region, induced by the intermolecular interactions between the FU and NA monomers. Existence of electronegative elements in these monomers facilitates their interactions through the H-bonding formation with the hydrogen atoms. Our findings show that dipole moment of the FU-NA complex in different solvents enhances as the dielectric constant increases. Hence, the highest dipole moments are observed in the polar solvents, whereas the smallest ones belonged to the non-polar solvents.

AIM Analysis

In order to obtain further insight into the nature of the H-bonds in the FU-NA complex, we have studied the electron density based on the topological parameters within the framework of Bader's theory of "Atoms in Molecules" [16,50,51]. The analysis of the electron density distribution is performed to find the bond critical points (BCPs) and to characterize them in terms of the electron density (ρ_{BCP}) and Laplacian ($\nabla^2\rho_{BCP}$) values. Based on the AIM theory, the Laplacian is negative for shared or polar interactions (covalent bonding) and it is positive for closed-shell interactions (H-bonds, ionic, van der Waals) [64,65]. The calculated topological parameters for FU-NA complex in the gas phase and the different solvents are summarized in Table 3.

As shown in Table 3, the maximum values of ρ and $\nabla^2\rho$ at the $O_{FU}\cdots H\text{-}C_{NA}$ and $O_{NA}\cdots H\text{-}N_{FU}$ H-bonds correspond to the FU-NA complex in the gas phase, while the minimum values of these parameters belong to the polar solvents. It is well known that the shorter distance can be attributed to the greater strength of the H-bond and the larger electron density (ρ) at the O···H contacts. The outcomes indicate that the minimum O···H contacts associated with the maximum electron densities at the O···H BCPs are observed for FU-NA complex in the gas phase. These outcomes observed are reversed for the related complex in the polar solvents. From the data obtained, it is concluded that the FU-NA complex in the gas phase has the strongest H-bond with respect to the solution phase (see Tables 1 and 3). The AIM calculations also indicate that the O···H bonds possess low ρ and the Laplacian of electronic density is positive at the BCPs of $O_{FU}\cdots H_{NA}$ ($\nabla^2\rho O_{FU}\cdots H_{NA}$) and $O_{NA}\cdots H_{FU}$ ($\nabla^2\rho O_{NA}\cdots H_{FU}$) bonds. Besides, the values of the virial atomic theorem (-V/T) in the presence of different solvents is equal to 2. Based on our theoretical results, the electronic charge is depleted in the interatomic path, indicating the closed-shell interactions. This means that the $O_{FU}\cdots H_{NA}$ and $O_{NA}\cdots H_{FU}$ bonds show electrostatic character in nature.

The average of the electron densities (ρ(Ω)), Laplacian of the electron density ($\nabla^2\rho(\Omega)$) and atomic electronic kinetic energy (K(Ω)) for atomic basins of O_{FU} and O_{NA} are also calculated upon complexation using AIM theory. The results are given in Table 3. These values are related to the electron density at the nuclear critical points. In the complex under study, the electron density for the O_{NA} basins is lower than that for the O_{FU} ones, indicating a more charge transfer from the O_{NA} basins to the $N\text{-}H_{FU}$. This result is in agreement with stronger H-bond energies of the $O_{NA}\cdots H\text{-}N_{FU}$ with respect to the $O_{FU}\cdots H\text{-}C_{NA}$. The obtained data also show that the greatest values of K(Ω) belong to FU–NA complex in the non-polar solvents in comparison to the polar ones (see Table 3). On the other hand, a meaningful relationship cannot be observed between the ρ(Ω) and $\nabla^2\rho(\Omega)$ values in the various solvents.

The contour map of FU-NA complex in the water solvent is displayed in Fig. 4. Interaction between FU and NA generates a cyclic system with a ring critical point (RCP) in intermolecular region. A RCP within the ring created is due to the formation of H-bonds. Furthermore, the $\nabla^2\rho_{RCP}$ is a point of the minimum electron density within

Table 3. Topological Parameters of FU-NA Complex in Different Solvents and the Average of these Values for Atomic Basins of O_{FU} and O_{NA} at the M06-2X/6-311++G(d,p) Level of Theory

Media	$O_{FU}\cdots H\text{-}C_{NA}$		$O_{NA}\cdots H\text{-}N_{FU}$						
	ρ	$\nabla^2\rho$	ρ	$\nabla^2\rho$	ρ_{RCP}	$\nabla^2\rho_{RCP}$	$\rho(\Omega)$	$\nabla^2\rho(\Omega)$	$K(\Omega)$
Water	0.0126	0.0435	0.0244	0.1104	0.0044	0.0173	8.8949	0.0012	75.4559
DMSO	0.0126	0.0435	0.0245	0.1106	0.0044	0.0174	8.8942	0.0004	75.4543
Methanol	0.0126	0.0435	0.0245	0.1107	0.0044	0.0174	8.8928	0.0011	75.4536
Ethanol	0.0126	0.0435	0.0245	0.1108	0.0044	0.0174	8.8931	0.0020	75.4547
Acetone	0.0126	0.0435	0.0246	0.1109	0.0044	0.0174	8.8936	0.0015	75.4545
Chloroform	0.0127	0.0440	0.0249	0.1124	0.0045	0.0176	8.8936	0.0010	75.4584
Ether	0.0127	0.0440	0.0250	0.1127	0.0045	0.0176	8.8926	0.0013	75.4578
Gas phase	0.0140	0.0502	0.0251	0.1136	0.0046	0.0180	8.8946	0.0023	75.4708

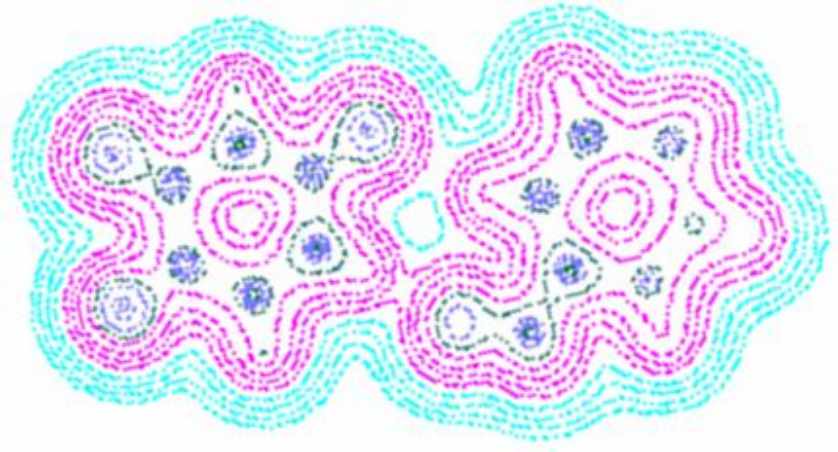

Fig. 4. The electron density contour map of FU-NA complex in the water solvent calculated at the M06-2X/6-311++G(d,p) level of theory using QTAIM.

the ring surface and a maximum on the ring line [66]. The results presented in Tables 1 and 3 indicate a linear relationship between the sum of H-bond energies (ΣE_{HB}) and the Laplacian of electron density at the RCP ($\nabla^2\rho_{RCP}$) with an excellent correlation coefficient (R is equal to 0.992). Therefore, ΣE_{HB} could be easily computed from $\nabla^2\rho_{RCP}$ with equation: $\Sigma E_{HB} = -4186.7\ (\nabla^2\rho_{RCP}) + 35.202$ (see Fig. 5). This indicates that the properties of the RCP values could be very useful in estimating the H-bonds strength.

NBO Analysis

Among theoretical methods, the natural bond orbital (NBO) analysis is a unique approach to evaluate

Table 4. NBO Analysis of FU-NA Complex, Occupation Numbers of Donor ($O.N._D$) and Acceptor ($O.N._A$) Orbitals, and the Energies (in kcal mol^{-1}) of some Important Orbitals

Media	$LPO_{FU} \rightarrow \sigma^*C\text{-}H_{NA}$			$LPO_{NA} \rightarrow \sigma^*N\text{-}H_{FU}$		
	$O.N._D$	$O.N._A$	$E^{(2)}$	$O.N._D$	$O.N._A$	$E^{(2)}$
Water	1.8541	0.0209	2.22	1.9754	0.0310	8.90
DMSO	1.8541	0.0209	2.23	1.9753	0.0311	8.93
Methanol	1.8540	0.0209	2.23	1.9753	0.0311	8.93
Ethanol	1.8540	0.0210	2.23	1.9753	0.0311	8.94
Acetone	1.8539	0.0210	2.23	1.9753	0.0313	8.96
Chloroform	1.8533	0.0211	2.30	1.9751	0.0313	9.08
Ether	1.8532	0.0212	2.32	1.9750	0.0313	9.10
Gas phase	1.8514	0.0220	2.62	1.9748	0.0310	9.28

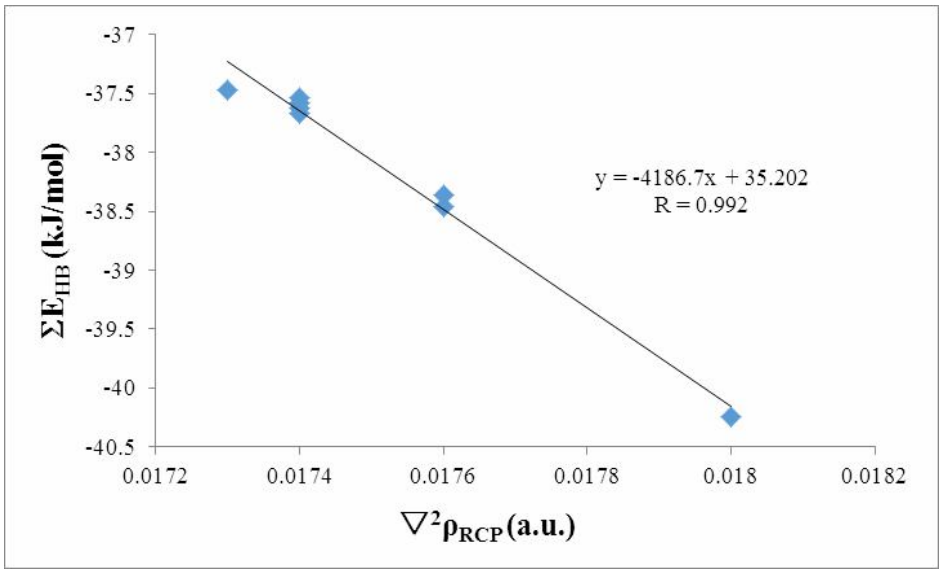

Fig. 5. Correlation between the sum of H-bond energies (ΣE_{HB}) *versus* the Laplacian of electron density at the RCP ($\nabla^2\rho_{RCP}$) at the M06-2X/6-311++G(d,p) level of theory.

the delocalization effects [67,68]. Table 4 shows the NBOs occupation number and the second-order perturbation stabilization energies, $E^{(2)}$, calculated at the M06-2X/6-311++G(d,p) level of theory. The obtained results confirm that the two H-bonds formed between FU and NA are related to the orbital interactions of the

$LPO_{NA} \rightarrow \sigma^*N\text{-}H_{FU}$ and $LPO_{FU} \rightarrow \sigma^*C\text{-}H_{NA}$. In the NBO analysis of the H-bond systems, the charge transfer between the lone pairs of proton acceptor and the anti-bonding orbitals of proton donor is of particular importance. For FU-NA complex, the charge is transferred from the lone pairs of FU and NA oxygen atoms to the anti-bonding orbitals of the C-H and N-H bonds of NA and FU, respectively. Our theoretical results also reveal that the occupation numbers of donor and acceptor orbitals in the polar solvents are approximately the same and do not change appreciably. From the obtained data, it is concluded that the polar solvents do not have a considerable effect on the H-bond of FU-NA complex. In addition, the consequences of NBO analysis show that the stabilization energies of $LPO_{NA} \rightarrow \sigma^*N\text{-}H_{FU}$ and $LPO_{FU} \rightarrow \sigma^*C\text{-}H_{NA}$ interactions decrease from the gas phase to the solution phase. The changes of stabilization energy for FU-NA complex in the polar solvents are the same for the $O_{FU}\cdots H\text{-}C_{NA}$ H-bond and relatively small for the $O_{NA}\cdots H\text{-}N_{FU}$ one. It is worth mentioning that the results of NBO support the outcomes achieved in the AIM framework [54,55,69].

In a NBO representation, for each donor NBO (i) and acceptor NBO (j), the stabilization energy $E^{(2)}$ associated with delocalization $i \rightarrow j$ is estimated as

$$E^{(2)} = -q_i \frac{F_{ij}^2}{\varepsilon_j - \varepsilon_i} \quad (4)$$

where q_i is the donor orbital occupancy, ε_i and ε_j are the diagonal elements (orbital energies of donor (i) and acceptor (j)) and F(i, j) is the off-diagonal NBO Fock matrix element [54,70]. The formation of a hydrogen bond implies that a certain amount of electronic charge is transferred from the proton-acceptor to the proton-donor molecule [71,72]. The charge transferred between the FU and NA monomers during complexation could be easily determined using Eq. (4). The values of charge transfer (q_{CT}) for the studied complex in the different solvents are listed in Table 5. As obviously seen in this Table, the largest charge transfer $|q_{(CT1)}|$ upon complexation is predicted in the gas phase, where the $q_{(CT1)}$ corresponds to the $O_{NA}\cdots H\text{-}N_{FU}$ H-bond. On the other hand, the theoretical calculations reveal that the maximum charge transfer value $|q_{(CT2)}|$ of the $O_{FU}\cdots H\text{-}C_{NA}$ H-bond corresponds to the water solvent in comparison with the other cases. As a result, the greater charge density on atoms involved in the H-bond leads to the more charge transfer of the FU-VB complex in the various solvents.

The effect of H-bond interactions on the Val_O occupation numbers of the FU-NA complex in different phases is also explored. As shown in Table 5, the Val_O occupation number in the gas phase is less than that in the solution phase. In other words, the Val_O occupancy increases in the presence of various solvents. For FU-NA complex, the hybridization of Lp_O corresponding to sp^n is also analyzed. The results obtained in this study show that the s character of O_{NA} orbital increases in the presence of different solvents with respect to the gas phase. The increment of s character in the related solvents leads to withdrawing the electrons and a decrease in the Lewis base (O atom) properties. This trend is reversed for the s character of O_{FU} orbital in the complex under study. However, these changes have an identical trend with the E_{HB}, ρ and $E^{(2)}$ values (related to $O_{FU}\cdots H\text{-}C_{NA}$).

Molecular Electrostatic Potential (MEP)

Figure 6 shows the MEP 3D plot of the FU-NA complex in the water solvent. The MEP is best suited for identifying the sites of intra- and intermolecular interactions [73,74]. It gives the visual representation of the chemically active sites and is a very useful descriptor in understanding the sites for the electrophilic and nucleophilic reactions as well as the H-bonding interactions. The different values of the electrostatic potential at the surface are presented by different colors. The red and blue areas in the MEP map refer to the electron-rich and electron-poor regions, respectively, whereas the green color signifies the neutral electrostatic potential. Potential increases in the order red < orange < yellow < green < blue.

In the present study, the MEP map shows that the negative potential site is on electronegative oxygen atoms and the positive potential site is around the hydrogen atoms. These sites give information about the region from where the compound can encompass intermolecular interactions. In fact, the O and H atoms involved in the H-bonding will be the most reactive sites for both regions of the H-bond-acceptor and H-bond-donor, respectively.

Table 5. The Results of NBO Analysis and the Charge Transfers (q_{CT} in e) at M06-2X/6- 311++G(d,p) Level of Theory

Media	Occ $ValO_{NA}$	Occ $ValO_{FU}$	S (%) O_{NA}	S (%) O_{FU}	$q_{(CT1)}$ $O_{NA}\cdots H\text{-}N_{FU}$	$q_{(CT2)}$ $O_{FU}\cdots H\text{-}C_{NA}$
Water	6.4663	6.6443	72.43	0.06	-1.9806	-1.9218
DMSO	6.4662	6.6441	72.42	0.06	-1.9873	-1.8375
Methanol	6.4661	6.6440	72.41	0.06	-1.9873	-1.8375
Ethanol	6.4660	6.6440	72.40	0.06	-1.9895	-1.8375
Acetone	6.4658	6.6440	72.39	0.06	-1.9940	-1.8375
Chloroform	6.4636	6.6436	72.22	0.06	-1.9805	-1.8952
Ether	6.4634	6.6436	72.20	0.06	-1.9848	-1.9116
Gas phase	6.4566	6.6427	71.77	0.08	-1.9987	-1.8745

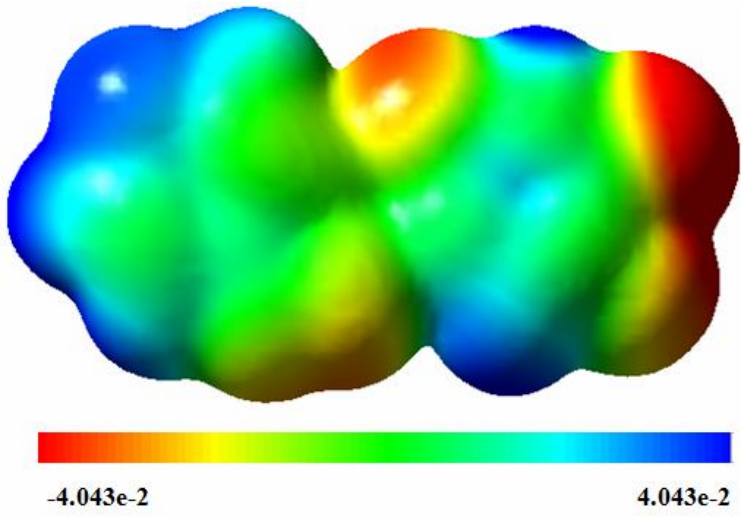

Fig. 6. Electrostatic potential of the FU-NA complex in the water solvent; color coding: red (very negative), yellow (slightly negative), light blue (positive) and dark blue (very positive).

CONCLUSIONS

In this study, the effect of different solvents on the stability order, binding energy and H-bond strength of FU-NA complex is investigated using the DFT calculations. Based on the average energies of the calculated H-bonds, the H-bond strength in the gas phase is higher than that in the solution phase. In the polar solvents, the H-bond energies are close to each other and lower than those in the non-polar solvents. Our findings also show that when the solvent effect is applied the binding energies of complex are significantly changed. Comparing the obtained binding

energies with the H-bond energies of the FU-NA complex in the various solvents shows a direct relationship between them. In other words, the results show that the binding energy of FU-NA complex in the polar solvents is lower than that in the non-polar ones, while it is higher in the solution than in the gas phase. Furthermore, in order to investigate the influence of solvent on the stability order of the FU-NA complex, the water is chosen as a natural compound of the cells to compare its effect with the other solvents. According to the obtained binding energies, the stability in the polar solvents is higher than that in the non-polar ones. Therefore, formation of FU-NA complex in ether, as a non-polar solvent, is more favorable with respect to other solvents, energetically. The AIM and NBO analyses are also carried out to gain further insight to the H-bonds strength. The AIM calculations indicate that the O···H bonds possess low ρ and the positive $\nabla^2\rho$ values, indicating the characteristic of the closed-shell interactions. The obtained results at the NBO basis are in accordance with the outcomes achieved in the AIM framework.

ACKNOWLEDGMENTS

The authors wish to thank Payame Noor University, Tehran, Iran, for their support.

REFERENCES

[1] P. Hobza, R. Zaradnik, Intermolecular Complexes: The Role of van der Waals Systems in Physical Chemistry and in the Biodisciplines, Elsevier, Amsterdam, 1988.

[2] I. Kaplan, Intermolecular Interactions: Physical Picture, Computational Methods and Model Potentials, John Wiley & Sons, Chichester, 2006.

[3] A. Campo-Cacharrón, A. Rodriguez-Sanz, E. Cabaleiro-Lago, J. Rodriguez-Otero, In 15th Int. Electron. Conf. Synth. Org. Chem., Vol. 15, MDPI, 2011.

[4] A.M. da Silva, A. Ghosh, P. Chaudhuri, J. Phys. Chem. A 117 (2013) 10274.

[5] G.A. Jeffrey, An Introduction to Hydrogen Bonding, Oxford University Press, New York, 1997.

[6] G.R. Desiraju, T. Steiner, The Weak Hydrogen Bond, in: Structural Chemistry and Biology, Oxford University Press, USA, 2001.

[7] A.D. Robertson, K.P. Murphy, Chem. Rev. 97 (1997) 1251.

[8] A. Ebrahimi, M. Habibi, H.R. Masoodi, Chem. Phys. Lett. 478 (2009) 120.

[9] A.J. Stone, The Theory of Intermolecular Forces, Clarendon Press, Oxford, 1997.

[10] A. Ebrahimi, H. Roohi, M. Habibi, L. Behboodi, J. Mol. Struct. 712 (2004) 159.

[11] S. Pasban, H. Raissi, F. Mollania, J. Mol. Liq. 215 (2016) 77.

[12] H. Roohi, A.R. Nowroozi, E. Anjomshoa, Comput. Theor. Chem. 965 (2011) 211.

[13] M. Yoosefian, A. Mola, J. Mol. Liq. 209 (2015) 526.

[14] M. Souri, A. Khan Mohammadi, J. Mol. Liq. 230 (2017) 169.

[15] F. Ravari, A. Khanmohammadi, Phys. Chem. Res. 3 (2015) 155.

[16] R.F.W. Bader, Atoms in Molecules: A Quantum Theory, Oxford University Press, New York, 1990.

[17] R.F.W. Bader, A. Bond Path: A universal indicator of bonded interactions, J. Phys. Chem. A 102 (1998) 7314.

[18] S. Vandhana, P.R. Deepa, G. Aparna, U. Jayanthi, S. Krishnakumar, Indian J. Biochem. Biophys. 47 (2010) 166.

[19] S. Wu, F. Li, X. Ma, M. Wang, P. Zhang, R. Zhong, Cytotoxicity of Eight Organic Solvents Towards Balb/3T3 and 293T Cells, IEEE, Wuhan, 2011.

[20] M. Timm, L. Saaby, L. Moesby, E.W. Hansen, Cytotechnology 65 (2013) 887.

[21] P.T. Jain, J.T. Pento, Res. Commun. Chem. Pathol. Pharmacol. 74 (1991) 105.

[22] L. Jamalzadeh, H. Ghafoori, R. Sariri, H. Rabuti, J. Nasirzade, H. Hasani, M.R. Aghamaali, Avicenna. J. Med. Biochem. 4 (2016) e33453.

[23] B.E. Reubinoff, M.F. Pera, C.Y. Fong, A. Trounson, A. Bongso, Nat. Biotechnol. 18 (2000) 399.

[24] J.M. Baust, R. Van Buskirk, J.G. Baust, *In Vitro* Cell. Dev. Biol. Animal 36 (2000) 262.

[25] D. McCabe, P. O'Dwyer, B. Sickle-Santanello, E. Woltering, H. Abou-Issa, A. James, Arch. Surg. 121 (1986) 1455.

[26] Z. Yan, J. Feng, J. Peng, Z. Lai, L. Zhang, Y. Jin, H. Yang, W. Chen, J. Lin, Oncol. Lett. 14 (2017) 7923.
[27] K. Abdi, Sh. Nafisi, F. Manouchehri, M. Bonsaii, A. Khalaj, J. Photochem. Photobiol. B: Biology 107 (2012) 20.
[28] R.T. Dorr, D.D. Von-Hoff, Cancer Chemotherapy Handbook, Appleton and Lange, Norwalk, 1994.
[29] K. Zare, F. Najafi, H. Sadegh, R. Shahryari Ghoshekandi, J. Nanostructure Chem. 3 (2013) 71.
[30] S.G. McDonald, E.S. Peterka, J. Am. Acad. Dermatol. 8 (1983) 107.
[31] D.M. Thappa, M. Senthilkumar, C. Laxmisha, Indian J. Sex. Transm. Dis. 25 (2004) 55.
[32] A. Shah, E. Nosheen, F. Zafar, S. Noman uddin, D.D. Dionysiou, A. Badshah, Z. ur-Rehman, G. Shahzada Khan, J. Photochem. Photobiol. B: Biology 117 (2012) 269.
[33] G.J. Peter, C.J. van Groeningen, Annals of Oncology 2 (1991) 469.
[34] P. Bachert, PROG. NUCL. MAG. RES. SP. 33 (1998) 1.
[35] B. Blicharska, T. Kupka, J. Mol. Struct. 613 (2002) 153.
[36] M.P. Findlay, M.O. Leach, Anti-cancer Drugs 5 (1994) 260.
[37] International Agency for Research on Cancer (IARC), Some N-Nitroso Compounds, IARC Monographs on the Evaluation of Carcinogenic Risk of Chemicals to Humans, Lyon, France, 1978.
[38] P.N. Magee, J.M. Barnes, Br. J. Cancer. 10 (1956) 114.
[39] R.C. Shank, P.N. Magee, Mycotoxins and N-nitroso Compounds: Environmental Risks, CRC Press, Florida, 1981.
[40] W. Lijinsky, Mutat. Res. 443 (1999) 129.
[41] H. Roohi, F. Akbari, Appl. Surf. Sci. 256 (2010) 7575.
[42] S.S. Hecht, Mutat. Res.-Fund. Mol. M. 424 (1999) 127.
[43] M.J. Frisch, G.W. Trucks, H.B. Schlegel, G.E. Scuseria, M.A. Robb, J.R. Cheeseman, J.A. Montgomery, Jr., T. Vreven, K.N. Kudin, J.C. Burant, J.M. Millam, S.S. Iyengar, J. Tomasi, V. Barone, B. Mennucci, M. Cossi, G. Scalmani, N. Rega, G.A. Petersson, H. Nakatsuji, M. Hada, M. Ehara, K. Toyota, R. Fukuda, J. Hasegawa, M. Ishida, T. Nakajima, Y. Honda, O. Kitao, H. Nakai, M. Klene, X. Li, J.E. Knox, H.P. Hratchian, J.B. Cross, V. Bakken, C. Adamo, J. Jaramillo, R. Gomperts, R.E. Stratmann, O. Yazyev, A.J. Austin, R. Cammi, C. Pomelli, J.W. Ochterski, P.Y. Ayala, K. Morokuma, G.A. Voth, P. Salvador, J.J. Dannenberg, V.G. Zakrzewski, S. Dapprich, A.D. Daniels, M.C. Strain, O. Farkas, D.K. Malick, A.D. Rabuck, K. Raghavachari, J.B. Foresman, J.V. Ortiz, Q. Cui, A.G. Baboul, S. Cli ‧ ord, J. Cioslowski, B.B. Stefanov, G. Liu, A. Liashenko, P. Piskorz, I. Komaromi, R.L. Martin, D.J. Fox, T. Keith, M.A. Al-Laham, C.Y. Peng, A. Nanayakkara, M. Challacombe, P.M.W. Gill, B. Johnson, W. Chen, M.W. Wong, C. Gonzalez, J.A. Pople, Gaussian 03, Revision A.7, Gaussian Inc., Pittsburgh, PA, 2003.
[44] Y. Zhao, D.G. Truhlar, Theor. Chem. Acc. 120 (2008) 215.
[45] J. Tomasi, M. Persico, Chem. Rev. 94 (1994) 2027.
[46] E. Cancès, B. Mennucci, J. Tomasi, J. Chem. Phys. 107 (1997) 3032.
[47] V. Barone, M. Cossi, J. Tomasi, J. Comp. Chem. 19 (1998) 404.
[48] E. Espinosa, E. Molins, C. Lecomte, Chem. Phys. Lett. 285 (1998) 170.
[49] S.F. Boys, F. Bernardi, Mol. Phys. 19 (1970) 553.
[50] C.F. Matta, R.J. Boyd, The Quantum Theory of Atoms in Molecules, Wiley, Weinheim, 2007.
[51] C.F. Matta and R.J. Boyd, Quantum Biochemistry, Wiley, Weinheim, 2010.
[52] K. Biegler, J. Schonbohm, R. Derdan, D. Bayles, R. Bader, AIM2000, Version 2.000, 2000.
[53] E. Glendening, A. Reed, J. Carpenter, F. Weinhold, NBO, version 3.1, Gaussian Inc, Pittsburg PA, CT, 2003.
[54] L. Hokmabady, H. Raissi, A. Khanmohammadi, Struct. Chem. 27 (2016) 487.
[55] F. Ravari, A. Khanmohammadi, Org. Chem. Res. 6 (2020) 36.
[56] Y.A. Abramov, Acta. Crystallogr. A 53 (1997) 264.
[57] Z. Desta, B.A. Ward, N.V. Soukhova, D.A. Flockhart, J. Pharmacol. Exp. Ther. 310 (2004) 1062.

[58] H. Raissi, M. Yoosefian, S. Khoshkhou, Comput. Theor. Chem. 983 (2012) 1.
[59] H. Raissi, F. Farzad, E.S. Nadim, M. Yoosefian, H. Farsi, A. Nowroozi, D. Loghmaninejad, Int. J. Quantum Chem. 112 (2012) 1273.
[60] H. Raissi, M. Yoosefian, F. Mollania, F. Farzad, A.R. Nowroozi, Comput. Theor. Chem. 966 (2011) 299.
[61] M. Yoosefian, Z. Jafari Chermahini, H. Raissi, A. Mola, M. Sadeghi, J. Mol. Liq. 203 (2015) 137.
[62] a) L. Onsager, J. Am. Chem. Soc. 58 (1936) 1486; b) J.G. Kirkwood, J. Chem. Phys. 3 (1935) 300.
[63] H. Raissi, A. Khanmohammadi, F. Mollania, Bull. Chem. Soc. Jpn. 86 (2013) 1261.
[64] M. Fazli, A.F. Jalbout, H. Raissi, H. Ghiassi, M. Yoosefian, J. Theor. Comput. Chem. 8 (2009) 713.
[65] H. Raissi, M. Yoosefian, F. Mollania, Int. J. Quantum Chem. 112 (2012) 2782.
[66] P. Popelier, Atoms in Molecules. An Introduction, Prentice-Hall Pearson Education Limited, Englewood Cliffs, NJ, 2000.
[67] F. Weinhold, in: P.v.R. Schleyer (Ed.), Encyclopedia of Computational Chemistry, Wiley, New York, 1998.
[68] H. Roohi, A.R. Noruozi, S. Salemi, J. Sharaki, J. Mol. Liq. 143 (2008) 119.
[69] A. Khanmohammadi, M. Mohammadi, J. Chil. Chem. Soc. 64 (2019) 4265.
[70] A.E. Reed, L.A. Curtiss, F. Weinhold, Chem. Rev. 88 (1988) 899.
[71] P. Hobza, Z. Havlas, Chem. Rev. 100 (2000) 4253.
[72] P. Hobza, V. Spirko, H.L. Selzle, E.W. Schlag, J. Phys. Chem. A 102 (1998) 2501.
[73] J.S. Murray, K. Sen, Molecular Electrostatic Potentials: Concepts and Applications, Elsevier, Amsterdam, 1996.
[74] E. Scrocco, J. Tomasi, In: P. Lowdin (Ed.), Advances in Quantum Chemistry, Academic Press, New York, 1978.